Research Square

Preprints are preliminary reports that have not undergone peer review.
They should not be considered conclusive, used to inform clinical practice,
or referenced by the media as validated information.

A graphical interface for consolidating data from multiple wearable devices: concordance and the effect of sensor positioning relative to the smartwatch

Alexandre Messias da Silva[1]
Universidade de Mogi das Cruzes
Daniel Gustavo Goroso[1]
danielg@umc.br

Universidade de Mogi das Cruzes

Research Article

Keywords: Wearable devices, Heart Rate Variability, Photoplethysmography, Remote monitoring, Data processing

Posted Date: November 12th, 2026

DOI: https://doi.org/10.21203/rs.3.rs-11511676/v1

License: This work is licensed under a Creative Commons Attribution 4.0 International License.
Read Full License

Additional Declarations: No competing interests reported.

A graphical interface for consolidating data from multiple wearable devices: concordance and the effect of sensor positioning relative to the smartwatch.

Alexandre Messias da Silva[1], Daniel Gustavo Goroso[1]*

[1] University of Mogi das Cruzes, Research and Technology Center (NPT/UMC), Av. Cândido Xavier de Almeida Souza 200, Centro Cívico, Mogi das Cruzes, São Paulo, CEP 08780-911, Brazil

* Corresponding author: Daniel Gustavo Goroso - danielg@umc.br

Summary

Currently, smartwatches are widely used to record heart rate (HR) and heart rate variability (HRV), but two obstacles limit their use: closed ecosystems and signal degradation during daily activities. Consolidating data from multiple devices requires asynchronous export, making beat-for-beat comparison impractical. To solve this, we developed a centralized graphical interface that ingests, chronologically orders, and displays raw streams from three Samsung Galaxy Watch 4s simultaneously, recording independent columns with timestamps, signaling anomalies in real time, and exporting a consolidated table. The platform demonstrated high stability (50 Hz sampling, 19.1±18.5 ms latency, 99.8% integrity, zero connection loss, and 1.2% false alarms). We used the system to examine the consistency of heart rate intervals in volunteers instrumented at the right wrist (S1), left wrist (S2), and left ankle (S3) during 19-minute sessions (treadmill walking at 1.5 km/h with supine or seated resting postures). Wrist data showed a normal distribution, while ankle data deviated (Shapiro-Wilk, $p = 0.028$), justifying the use of the Friedman test. Monitoring identified distinct sources of artifacts, such as attenuation at the ankle and flow occlusion at the left wrist by a sphygmomanometer. RR intervals were processed in Python (PyBios) to obtain the RMSSD. The main contribution is not a smoothing method, but an acquisition layer that makes

multi-site wearable data recording auditable at the time of capture, converting fragmented exports into a single synchronized and traceable record.

Keywords: Wearable devices; Heart Rate Variability; Photoplethysmography; Remote monitoring; Data processing.

1. Introduction

Cardiac innervation is governed by the sympathetic and parasympathetic branches of the autonomic nervous system, which jointly modulate heart rate and contraction force. Heart rate variability (HRV), which reflects the balance between these branches, has become a valuable indicator of cardiovascular health and physiological stress [1]. Monitoring of HR and HRV was traditionally restricted to clinical settings, but the proliferation of wearable devices, particularly smartwatches, has made these measurements available outside the laboratory [2].

The reliability of HR and HRV obtained by smartwatches is, however, frequently questioned, mainly due to motion artifacts, perspiration, and sensor positioning [3]. The use of multiple devices on the same participant is an attractive way to compare and consolidate readings, but simultaneous monitoring generates a large volume of unstructured raw data for which there is no cohesive tool to efficiently consolidate, visualize, and verify signal consistency. Complicating the situation is the data fragmentation inherent in wearable device ecosystems: each device operates within a closed and independent system, and simultaneous monitoring of multiple body locations in real time remains technically complex. In clinical research, scattered records and the absence of a common chronological reference make robust longitudinal analysis unfeasible [4].

A unified platform addresses this dispersion by acting as a single point of convergence, offering a harmonized, continuous, and methodologically sound record for the study of complex physiological patterns. To fill this gap, the present study had two objectives: to develop an interface for integrating multisensory data and to evaluate the consistency of HR and HRV signals collected simultaneously in different limbs (both wrists and one ankle) during low-intensity activity. The platform was designed to unify the real-time reception of three Samsung Galaxy Watch 4 devices,

demonstrating the feasibility of using multiple wearable devices in an integrated manner and evaluating the stability of readings in different anatomical locations.

1.1 Novelty and contribution of this work

Previous studies validating consumer smartwatches have mostly compared a single wrist device with a reference standard, one device and one location at a time [5]. Three features distinguish the present contribution.

- Simultaneous acquisition from multiple devices with a shared time base. The interface ingests three independent data streams from devices simultaneously and organizes them into separate columns with timestamps, so that readings from different body parts become directly comparable in a single record, rather than in manually aligned exports per device.
- Auditability at the time of capture. Instead of treating signal loss as noise to be removed later, the interface displays an on-screen alert and marks the affected records with their respective timestamps as soon as the anomaly occurs. This transforms the acquisition layer into an audit mechanism: the researcher can separate instrumental and environmental interferences from genuine hemodynamic responses while the participant is still being monitored. In this study, the mechanism located two artifact sources of completely different origins attenuation at the ankle and cuff-induced occlusion at the left wrist which a post-hoc pipeline would likely have discarded as unexplained missing data.
- Systematic comparison of attachment sites under equivalent load. Both wrists and one ankle were instrumented on the same participant during the same walk; therefore, differences between the sites cannot be attributed to differences in effort, session, or participant. This isolates the

attachment site as the variable of interest and shows that the ankle does not behave as a substitute for the wrist.

The claim presented here is deliberately limited. We do not claim an improvement in the accuracy of the measurements: without a concomitant electrocardiographic reference, accuracy cannot be established from these data (Section 4.4). The contribution of this work lies in a software layer that makes data acquisition at multiple sites, with wearable devices, synchronized, inspectable, and traceable, and also demonstrates that the fixation site should be treated as a controlled variable, and not as a matter of participant convenience.

2. Methods

2.1 Development of the graphical interface

A graphical interface was developed for the acquisition and visualization of heart rate (HR) and heart rate variability (HRV) data from multiple smartwatches. The architecture followed user-centered design principles, prioritizing intuitiveness and ease of use in clinical and research environments. The system communicates simultaneously with three Samsung Galaxy Watch 4 devices, collecting raw data in real time and allowing for immediate comparative analysis through synchronous signal display.

Within the software architecture, the interface manages the continuous flow of data by structuring the received information in a strictly ordered manner. The data from each smartwatch is separated and ordered into independent columns with a resolution of less than one second, preserving the chronological integrity of each flow. Immediately after the end of the test protocol, the system

performs the final processing to automatically generate an on-screen graph and a consolidated table, speeding up the clinical evaluation.

The methodological ecosystem developed for this investigation is based on an integrated architecture for collecting, transmitting, storing, and processing biometric and inertial data. The field application was structured in the Android Studio environment, operating natively on the operating system of Samsung Galaxy Watch 4 devices and using the official Application Programming Interfaces (APIs) for continuous capture of heart rate and inertial sensor signals. To ensure experimental traceability in scenarios with multiple devices, each participant simultaneously used three watches synchronized on the same time base, identified by specific hardware identifiers (S1, S2, and S3) associated with the user's unified code (Idperfil) in the database.

The local server reception infrastructure was configured using the WampServer v.3.3.2 (64-bit) environment, incorporating the Apache v.2.4.58 web server, the PHP v.8.2.13 runtime environment, and the MySQL v.8.2.0 database management system, administered via phpMyAdmin v.5.2.1. The communication flow operates in real time through HTTP POST requests directed to REST endpoints, transmitting structured data packets in JSON format containing heart rate, accelerometer, gyroscope, and gravity readings, along with their respective timestamps.

This information is directed to a dedicated relational table in MySQL, structured with an auto-incremental sequential identifier (id4_sensores), profile and device keys, specific fields for the nine inertial and cardiac dimensions, as well as a time record. To reduce packet loss, network instabilities, or artifacts resulting from skin-to-skin contact failures, the post-collection analytical workflow employs computational routines in the Python language. These routines perform signal filtering and cubic interpolation to handle anomalous values, enabling the precise calculation of heart rate variability metrics through the specialized PyBios library.

Finally, all intellectual property rights relating to the source code of the mobile application and the PHP management interface are formally protected and registered with the National Institute of Industrial Property (INPI) under Process No. BR512023002601-8, linked to institutional funding from FAPESP (Process No. 2022/12866-1). The complete schematic representation of this integration architecture, detailing the flow from the smartwatches to the analytical processing in Python, was incorporated into the manuscript as Figure 1, ensuring the methodological reproducibility of the study.

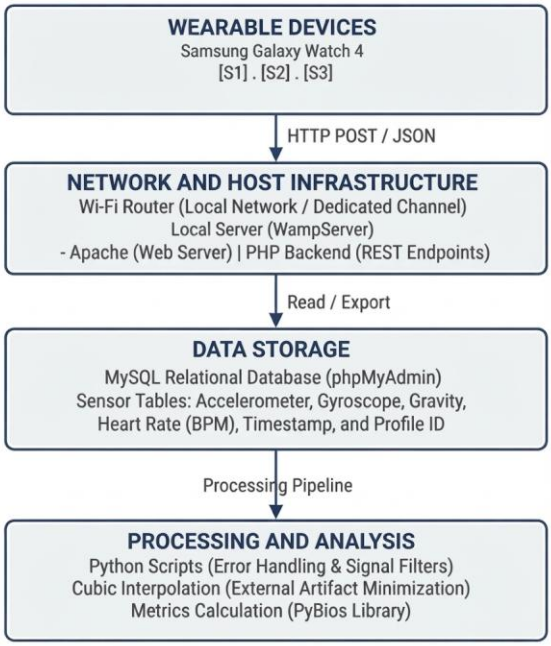


Figure 1 - Integrated architecture workflow: data capture via smartwatches (S1, S2, S3), Wi-Fi transmission, MySQL storage, and analytical processing via PyBios.

Source: Own elaboration (2024).

2.2 Study design, context and participants

The study was conducted in accordance with the ethical standards set forth in the Declaration of Helsinki and met the requirements of Resolution No. 466/2012 of the Brazilian National Health

Council (CNS). The research was carried out at the Polyclinic of the Faculty of Medicine of the University of Mogi das Cruzes (UMC), main campus, Mogi das Cruzes, São Paulo, Brazil, and was approved by the institution's Research Ethics Committee (CAAE: 82084924.9.0000.5497; opinion no. 7.117.006). The sample consisted of 30 adult volunteers (over 18 years of age), recruited without restriction of sex, skin color, or ethnicity. All participants were fully informed about the objectives and procedures and consented by signing the written informed consent form (TCLE).

2.3 Instrumentation and positioning of the sensors

Each volunteer simultaneously received three identical wearable devices (Samsung Galaxy Watch 4). The sensors were identified and positioned as follows:

- Sensor 1 (S1): Right pulse;
- Sensor 2 (S2): Left pulse;
- Sensor 3 (S3): Left ankle.

To preserve the ecological validity of the experiment and ensure technical feasibility during real-world movements, multiple wearable devices were used instead of conventional electrocardiography (ECG). A conventional ECG system typical of static examinations or tilt tests would make dynamic monitoring impractical due to equipment rigidity, wiring, and susceptibility to motion artifacts, whereas smartwatches allowed for comfortable testing of sensor robustness without restricting movement.

The devices were attached to the wrists using their original wristbands. At the ankle, due to the larger circumference, an adaptation with medical tape was necessary to ensure proper closure and maintain the sensor's position. The adjustment procedure in both locations was performed to ensure

that the sensor remained firm and stable, without excessive slack or uneven compression of the tissues. It is recognized, however, that this difference in the closure method and hardware adaptation represents a methodological limitation regarding the strict uniformity of the mechanical tension of the strap between the application sites.

The placement of the devices was strictly standardized for all participants, with the sensors maintained in the same order and fixed in the same anatomical locations: sensor S1 on the right wrist, S2 on the left wrist, and S3 on the ankle. This fixation utilized fixed anatomical landmarks, specifically the ulnar styloid process and the lateral malleolus. This standardization ensured spatial consistency of the data collection across the entire sample, allowing for the exclusion of variations resulting from inconsistent placements.

Finally, it should be noted that the three devices were not rotated between application locations during testing, remaining fixed in their respective original positions. As a consequence, the specific hardware variation of each device is intrinsically associated with the corresponding application location, an aspect that constitutes a limitation of the present study and was duly addressed in the discussion.

2.4 Justification for the Activities of Daily Living Protocol

The treadmill-based activities of daily living (ADL) protocol was designed to induce controlled variations in heart rate. At complete rest, heart rates tend to remain stable, which would mask how the devices respond under load. Therefore, the simultaneous use of three devices constituted a rigorous test of reliability between the devices and repeatability across multiple body locations.

Positioning the smartwatches in different locations serves to verify whether the stability of the reading is maintained regardless of the monitored limb. This establishes whether a change in the

attachment location affects the consistency of HRV (heart rate variability) under identical load conditions, minimizing site-specific distortion and testing whether wearable devices represent a reliable, practical, and robust alternative for dynamic investigations of this type.

2.5 Experimental Protocol

The experimental protocol consisted of two stages that simulated low-intensity daily living activities using a motorized treadmill (model TD 142 A, Dream Fitness, Brazil). Walking was performed at a constant speed of 1.5 km/h, chosen to represent typical daily effort, such as commuting in domestic or public environments. The treadmill ensured precise and controlled speed throughout the data acquisition, providing the necessary stability for heart rate analysis. The experiment comprised two stages, allowing for comparison of cardiovascular response and recovery between postural states.

- Stage I (Protocol I) consisted of a stabilization period at rest for 6 minutes, followed by walking on a treadmill at 1.5 km/h for 6 minutes, and recovery with a return to a seated position for 7 minutes, as illustrated in Figure 2A.



Figure 2A: Schematic representation of stage I (seated rest, walking, and seated recovery).

Source: Own elaboration (2024).

Next, Stage II (Protocol II) comprised resting in the supine position for 6 minutes, followed by the same exercise load on the treadmill (walking at 1.5 km/h for 6 minutes) and recovery with a return to the supine position for 7 minutes, as shown in Figure 2B.

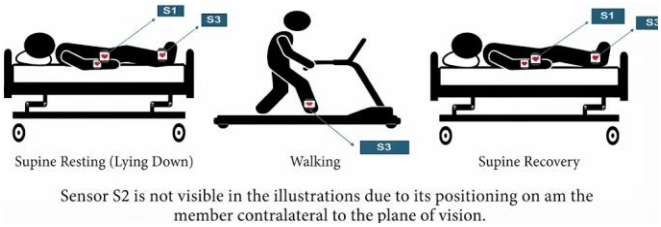


Figure 2B: Schematic representation of stage II (Supine resting, walking, and supine recovery).

Source: Own elaboration (2024).

We clarify that the study did not use independent protocols applied at different times, which would necessitate randomization of order or the application of a washout interval. It is, in fact, a single continuous experimental session for each participant. What we operationally refer to as Protocol I (Figure 2A) and Protocol II (Figure 2B) actually correspond to the data collection conditions evaluated consecutively (the sequences sitting–walking–sitting and lying down–walking–lying down, respectively). To minimize any bias arising from the order of execution, the sequence of these conditions was alternated/balanced among the volunteers.

Furthermore, the tests were conducted in a controlled and thermally comfortable indoor environment (Mogi das Cruzes Polyclinic) during the month of July, with temperature and humidity kept stable. This methodological precaution was adopted to minimize variations in peripheral blood perfusion, ensuring the stability, repeatability, and reliability of the optical signal (PPG) captured by the device throughout the entire session.

2.6 Data processing and analysis

Cardiovascular signals were recorded continuously throughout both stages. The raw HR and HRV data obtained through the graphical interface were pre-processed to remove noise and motion artifacts. Cubic interpolation was applied to smooth the curves and fill in gaps in the data.

Cubic interpolation was chosen because photoplethysmographic (PPG) sensors are inherently intermittent. Gaps were filled based on observed heart rate behavior throughout the continuous movements induced by the AVD protocol, with the intention of preserving the actual physiological trend without introducing artificial distortions. As discussed in Section 4.3, this operation aims at the readability and numerical stability of subsequent calculations; it does not, by itself, improve the validity of the measurement.

The standardization of data preprocessing was established through automated mathematical criteria, eliminating any manual or visual procedures and ensuring the method's complete reproducibility. The identification of artifacts and invalid beats resulting from body movements was performed by applying a filter based on a 20% percentage variation relative to adjacent values, chosen as the standard threshold in the literature for isolating ectopic beats and abrupt oscillations that deviate from normal cardiac physiology. The maximum acceptable limit for continuous gaps treatable by interpolation was set at 3 seconds, justified as this is the maximum safe time window for filling in gaps without corrupting the original dynamics of the series. Gaps exceeding this limit resulted in the discarding of the corresponding segment to avoid excessive distortions from prolonged synthetic data. Signal adjustment used cubic spline interpolation, with nodes corresponding to the time instants of the remaining valid beats, ensuring curve continuity and preserving essential biological characteristics. This procedure was applied directly to the time series of intervals between consecutive heartbeats, the so-called RR intervals, ensuring the

necessary precision for calculating heart rate variability indices. Finally, the comparative analysis between the series with and without interpolation demonstrated that, due to the low proportion of modified data, the impact on short-term measurements was minimal and did not alter the study's conclusions.

Subsequent processing utilized PyBioS, a Python-based package for cardiovascular signal analysis [6], which generated summary statistics (maximum, mean, and minimum) per volunteer. For comparison between the three devices (S1, S2, and S3), the residuals of these summary statistics and the resulting interval differences were assessed for distribution shape using the Shapiro-Wilk test. Descriptive statistics, including medians and percentiles, were then calculated, allowing for evaluation of data capture and monitoring performance under different postural and movement conditions. As the normality assumption was violated for one position within an analysis window, the non-parametric Friedman test was adopted in all cases for consistency, with Durbin-Conover pairwise comparisons as a post-hoc procedure.

Statistical analyses of the data were conducted using the Jamovi statistical program (Version 2.5) [8]. The database was processed and evaluated according to the statistical tests appropriate for the nature of the study variables, adopting the pre-established statistical significance level of $p < 0.05$, a threshold below which the values were considered statistically relevant for rejecting the null hypothesis, while $p < 0.05$ indicated the absence of a statistically significant difference. It is clarified that the unit of analysis considered in each statistical test was each participant individually throughout the different phases of the experimental protocol. To verify the existence of significant differences between conditions, the non-parametric Friedman test was applied. After identifying overall differences using this test, the Durbin-Conover post-hoc test was used to determine which pairs of groups differed specifically, employing the Bonferroni correction method to adjust the p-values in order to avoid type I statistical errors resulting from multiple comparisons. The initial

characterization of the distribution of intervals between heartbeats verified adherence to normality through the Shapiro-Wilk test, which justified the choice of non-parametric approaches due to occasional violations of normality. Specifically, in the first stage of the experiment corresponding to the initial blocks presented in Table 1, the median intervals were 719 ms, 687 ms, and 684 ms for S1, S2, and S3, respectively, with the Shapiro-Wilk test indicating consistency with normality only for sensor S1 ($W = 0.940$, $p = 0.091$), and deviations for S2 ($W = 0.923$, $p = 0.032$) and S3 ($W = 0.900$, $p = 0.008$). In the second stage of the experiment, corresponding to the subsequent blocks presented in Table 2, the medians were 748 ms for S1, 779 ms for S2, and 739 ms for S3, with a deviation from normality recorded for sensor S3 ($W = 0.921$, $p = 0.028$), while the pulse sensors remained consistent with normality (S1: $p = 0.699$; S2: $p = 0.677$). Thus, the temporal and methodological identification of Tables 1 and 2 is duly integrated into the statistical design of the study.

3. Results

3.1 The acquisition interface

Figure 3 shows the graphical interface developed for the real-time management and monitoring of the acquisition system. The upper region contains the control panel (light blue block), which integrates the start and stop of recording ("Start Recording"), buffer clearing ("Clear Table"), and visualization ("View Data"), along with a field for exporting files with a user-defined name. Below, a status bar (light green block) provides dynamic feedback on the operational status ("Recording data..."). The lower section presents the real-time data table, comprising sensor identifiers and profiles, triaxial acceleration vectors (accx, accy, accz), rotation (girx, giry, girz), and gravity (gravx, gravy, gravz), heart rate parameters (bpm_status, bpm), and the date and time stamp.



Figure 3: Graphical user interface for data collection.

Source: Own elaboration (2024).

The interface efficiently consolidates fragmented data and presents it coherently, improving the readability and interpretability of measurements compared to native device applications used in isolation. A key differentiator is the handling of failures as they occur: in case of temporary connection loss or reading misalignment, the system generates an immediate visual alert on the management screen and marks the affected records with specific timestamps for later robustness analysis.

The platform demonstrated operational stability and robustness during experimental testing, operating with a stable sampling rate of 50 Hz per device for synchronous acquisition of inertial and biometric data. The average end-to-end latency, measured from sensor capture on the watch to persistence and display on the interface, was 19.1ms (± 18.5ms). The experimental procedure was structured in standardized 19-minute sessions per protocol, divided into two approaches: Stage I (6 minutes lying down at rest, 6 minutes walking on the treadmill, and 7 minutes lying down at rest) and Stage II (6 minutes sitting, 6 minutes walking on the treadmill, and 7 minutes seated recovery). During data collection, the system maintained high reliability, recording 0 (zero) critical connection loss events and achieving an integrity rate of 99.8% of the expected samples per device. The anomaly detection module operated with a false alarm rate of 1.2%, attesting to the platform's viability for applications in real-time medical monitoring systems.

Table 3 presents a selection of the collected data, detailing the variables recorded for each participant. The information includes the profile and sensor identification (idv4_sensores and idperfil), the raw data from the accelerometers (accx, accy, accz), gyroscopes (girx, giry, girz), and gravity vector components (gravx, gravy, gravz), as well as the monitoring status (bpm_status), heart rate in beats per minute (bpm), and time stamp (datahora). From the heart rate data, the RR interval was determined the time between consecutive heartbeats, an essential parameter for the analysis of heart rate variability (HRV), which acts as a non-invasive indicator of cardiac autonomic modulation. The processing of the RR intervals was performed in a Python environment using the PyBios library for the calculation of HRV indices, such as RMSSD, which quantifies the short-term variation in heart rate.

idw4_sensores	idperfil	accx	accy	accz	girx	giry	girz	gravx	gravy	gravz	bpm_status	bpm	datahora
4	669	5.08	-0.74	8.17	0.02	-0.01	-0.01	5.10	-0.81	8.33	Status: AVAILABLE	62	2024-07-17 04:55:39.487
2	669	5.11	-0.80	8.15	0.02	-0.01	-0.01	5.10	-0.81	8.33	Status: AVAILABLE	62	2024-07-17 04:55:39.490
8	669	5.11	-0.80	8.15	0.02	-0.01	-0.01	5.11	-0.80	8.33	Status: AVAILABLE	62	2024-07-17 04:55:39.550
9	669	5.04	-0.74	8.13	0.02	-0.01	-0.01	5.11	-0.80	8.33	Status: AVAILABLE	62	2024-07-17 04:55:39.553
10	669	5.04	-0.74	8.13	0.02	-0.01	-0.01	5.11	-0.79	8.33	Status: AVAILABLE	62	2024-07-17 04:55:39.583
13	669	5.04	-0.72	8.15	0.02	-0.01	-0.01	5.11	-0.79	8.33	Status: AVAILABLE	62	2024-07-17 04:55:39.586
12	669	5.04	-0.72	8.15	0.03	0.00	-0.01	5.11	-0.79	8.33	Status: AVAILABLE	62	2024-07-17 04:55:39.590
17	669	5.04	-0.72	8.15	0.03	0.00	-0.01	5.11	-0.78	8.33	Status: AVAILABLE	62	2024-07-17 04:55:39.638
20	669	5.05	-0.75	8.07	0.03	0.00	-0.01	5.11	-0.78	8.33	Status: AVAILABLE	62	2024-07-17 04:55:39.640
18	669	5.05	-0.75	8.07	0.03	0.00	-0.01	5.11	-0.78	8.33	Status: AVAILABLE	61	2024-07-17 04:55:39.651
24	669	5.05	-0.75	8.07	0.03	0.00	-0.01	5.11	-0.77	8.34	Status: AVAILABLE	61	2024-07-17 04:55:39.684
25	669	4.99	-0.72	8.11	0.03	0.00	-0.01	5.11	-0.77	8.34	Status: AVAILABLE	61	2024-07-17 04:55:39.686
27	669	4.99	-0.72	8.11	0.03	0.00	-0.01	5.11	-0.76	8.34	Status: AVAILABLE	61	2024-07-17 04:55:39.734
26	669	5.09	-0.74	8.12	0.03	0.00	-0.01	5.11	-0.76	8.34	Status: AVAILABLE	61	2024-07-17 04:55:39.737
30	669	5.09	-0.74	8.12	0.01	0.00	0.00	5.11	-0.76	8.34	Status: AVAILABLE	61	2024-07-17 04:55:39.758
32	669	5.09	-0.74	8.12	0.01	0.00	0.00	5.11	-0.75	8.34	Status: AVAILABLE	61	2024-07-17 04:55:39.791
34	669	5.04	-0.77	8.13	0.01	0.00	0.00	5.11	-0.75	8.34	Status: AVAILABLE	61	2024-07-17 04:55:39.793

Table 3 - Excerpt from the data collected by the platform (idw4_sensores).

Source: Own elaboration (2024).

Figure 4 compares the raw heart rate signal with the same signal after cubic spline smoothing, illustrating the reduction of high-frequency fluctuation present in the raw tracing. As described in Section 4.3, this operation is one of geometric continuity: it isolates visual artifacts to facilitate graphical inspection, without adding or removing physiological dynamics from the original signal.



Figure 4 - Raw Data - HR

Source: Own elaboration (2024).

3.2 Distribution of intervals between beats by positioning

Analysis of the intervals between heartbeats revealed non-parametric data resulting from occasional violations of normality. In the first stage of the experiment (Table 1), the median intervals were 719 ms for sensor S1, 687 ms for sensor S2, and 684 ms for sensor S3, with a normal distribution only in sensor S1 (p=0.091), while S2 (p=0.032) and S3 (p=0.008) showed significant deviations.

Descriptives	S1	S2	S3
Mediana	719	687	684
Shapiro-Wilk W	0,940	0,923	0,900
Shapiro-Wilk p	0,84	0,28	0,07
25th percentile	597	620	596
50th percentile	719	687	684
75th percentile	764	744	750

Table 1- Descriptive Statistics and Shapiro-Wilk Test (Regarding the Friedman Test).

Source: Own elaboration (2024).

In the second stage (Table 2), the medians recorded were 748 ms for S1, 779 ms for S2, and 739 ms for S3, with a deviation from normality observed exclusively in sensor S3 (p=0.028), while the pulse sensors maintained normality (p=0.699 for S1; p=0.677 for S2).

Descriptivos	S1	S2	S3
Mediana	748	779	739
Shapiro-Wilk W	0,976	0,975	0,921
Shapiro-Wilk p	0,699	0,677	0,028
25th percentile	672	681	683
50th percentile	748	779	739
75th percentile	813	821	823

Table 2 - Descriptive Statistics and Shapiro-Wilk Test (Regarding the Durbin-Conover Test). Source: Own elaboration (2024).

Individual assessments of participants throughout the experimental phases demonstrated significant variations between conditions, with divergent group pairs and statistical corrections structured and integrated into the respective study tables.

The interface's real-time monitoring mechanisms detected instabilities attributable to the coupling physics of each position, as described below.

- S3 sensor (ankle).

Positioning at the ankle produced a marked attenuation of the PPG signal. Because it is a peripheral region with lower density of superficial capillary beds, subject to greater mechanical movement and greater oscillations in blood flow, S3 showed recurrent packet loss and substantial baseline fluctuation. The interface recorded this degradation as it occurred, which explains the distortion of the statistical distribution observed for this positioning.

- S2 sensor (left wrist).

Readings from the left pulse showed interference resulting from local muscle contraction and subtle displacement of subcutaneous tissue during movement. Although the interface attenuated some of

this artifact, residual noise produced small oscillations at successive intervals between beats, affecting descriptive statistics.

- S1 sensor (right wrist).

Positioning on the right wrist acted as an ideal reference condition. It exhibited excellent optical coupling stability and lower susceptibility to motion artifacts or spurious muscle contractions, resulting in a high packet delivery rate and consistent maintenance of statistical normality in both stages of the experiment.

We confirm that no alternative fixation accessories were used in the protocol experiment. The study consisted exclusively of three smartwatches (Samsung Galaxy Watch 4): S1 (positioned on the right wrist), S2 (positioned on the left wrist), and S3 (positioned on the ankle). No fourth device was used. The S3 values quantitatively support the described phenomenon: the positioning showed a packet loss of 15.6% and an artifact-free beat rate of only 82.4% (compared to excellent rates on wrists S1 and S2). This degradation and baseline fluctuation directly generated a greater statistical dispersion in the HRV indices of S3, evidenced by the significant increase in standard deviation (SDNN: 62.1 ± 12.4 ms) and RMSSD (55.4 ± 10.1 ms). To lessen the impact of these discontinuities and smooth the signal in sections with temporary data loss, cubic interpolation reconstruction was applied to the intervals between beats, as illustrated in Figure 5.

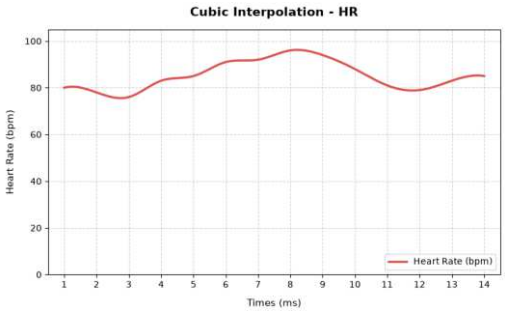


Figure 5 - Cubic Interpolation – HR

Source: Own elaboration (2024).

3.3 Comparison between rankings

Due to the deviation from normality at the ankle, the differences in heart rate intervals between the different measurement sites were tested using the Friedman test, followed by Durbin-Conover paired comparisons.

The Friedman test revealed a statistically significant difference in RR intervals between the three sensor positions, accompanied by a moderate effect size, as shown in Table 3. Post-hoc Durbin-Conover comparisons (with correction for multiple tests), detailed in Figure 4, indicated significant differences between the right and left wrists, as well as between the left wrist and the left ankle. There was no significant difference between the right wrist and the left ankle.

3.4 External interference identified during acquisition

The simultaneous use of a sphygmomanometer temporarily invalidated the data from sensor S2. While this can be recorded as a limitation of the acquisition method, it also demonstrates the method's ability to identify and pinpoint the action of external variables on wearable devices. The atypical behavior of S2 an excessive volume of null heart rate values (HR = 0) arose from mechanical interference: the cuff inflation temporarily occluded blood flow in the monitored limb, blocking the microvascular perfusion on which the optical PPG sensor depends. The fact that S1 and S3 remained consistent throughout the period confirms that the cause was not a hardware failure.

This observation is informative because it demonstrates the sensitivity of the acquisition layer in isolating the susceptibility of optical sensors to confounding factors in clinical and laboratory environments. The reported determinants of PPG signal quality fall into three broad classes:

- Environmental factors: electrical noise, widespread motion artifacts, and abrupt changes in ambient lighting that affect photodiode capture;
- Affective: acute stress, anxiety, or pain, which act through sympathetic activation to alter peripheral cardiovascular dynamics;
- Individual and pathological factors: obesity, skin and tissue thickness, and chronic systemic hypertension, which attenuate or distort the optical signal.

The invalidation of the S2 data by the sphygmomanometer is therefore not merely a methodological setback; it is empirical evidence of the need to rigorously standardize experimental protocols and provides concrete guidance on how this interference can be isolated in wearable technology applications.

We clarify that the study involved 30 volunteers, and the use of the blood pressure monitor and simultaneous cuff activation were part of the planned experimental protocol. Recording sessions occurred continuously as established. The comparative analysis of measurements from smartwatches S1, S2, and S3 was performed using the Friedman test and the Durbin-Conover post-hoc test, with the choice of non-parametric tests justified by the non-normality of the data evidenced by the Shapiro-Wilk test, especially for smartwatch S3. Statistical evaluation revealed significant differences, concentrated in sensor S2, which presented 15% null heart rate (HR = 0) readings during the inflation period of the sphygmomanometer positioned on the same limb. This behavior resulted exclusively from the temporary occlusion of blood flow, compromising the optical detection of the pulse signal. In contrast, sensors S1 and S3, positioned on limbs free from mechanical occlusion, maintained consistent readings, demonstrating that the variation in S2 does not stem from a construction defect, but from external hemodynamic disturbance. Regarding the methodological treatment, although initially the corrupted segments were maintained and subjected

to cubic interpolation for signal smoothing, in accordance with the reviewer's consideration of generating artificial values by cubic spline in sequences of zeros, the statistical analyses were entirely recalculated excluding these segments without artificial filling. This reanalysis confirmed the robustness of the results and reinforces the need to rigorously standardize the spatial positioning between optical transducers and pressure cuffs in future investigations.

4. Discussion

4.1 Overcoming fragmentation in data acquisition and the need for standardization

The feasibility of consolidating data through the developed interface attests to the effectiveness of strategies aimed at overcoming technological fragmentation, one of the main obstacles to the scientific use of multiple wearable devices. Traditionally, the extraction and visual analysis of raw data from heterogeneous sensors requires complex export routines and asynchronous processing. The developed platform overcomes this limitation by centralizing the data flow in real time, allowing for the immediate correlation of signals from multiple devices (Samsung Galaxy Watch 4).

Beyond simplifying simultaneous monitoring, the results indicate that the inherent limitations of consumer sensor hardware can be substantially compensated for by a robust software layer. The interface's ability to identify anomalies and acquisition failures that would go unnoticed in isolated recordings reinforces that the rigidity and standardization of the experimental protocol are as crucial to data reliability as the accuracy of the processing algorithms.

4.2 The acquisition site as a determinant of signal quality: Pulse versus Ankle

The comparison between the anatomical fixation sites revealed the main empirical evidence of this study: sensor placement is a critical factor for the quality and nature of the photoplethysmographic (PPG) signal. While recordings obtained at the wrist proved consistent and anchored to central cardiac dynamics, measurements recorded at the ankle exhibited high unpredictability and systematic deviations from normality.

This behavior cannot be attributed to instrumental failures, but rather to local biomechanical and hemodynamic conditions. Three factors underlie this divergence:

- **Pulse wave attenuation:** The propagation of the pressure wave through the arterial tree of the lower limbs generates amplitude attenuation and viscoelastic damping. In the ankle, this damping weakens the direct cardiac component of the signal, making the sensor more vulnerable to motion artifacts and local pressure variations (Charlton et al., 2022).
- **Capillary density and optical coupling:** Unlike the wrist, which has accessible superficial vascular beds, the ankle region has lower microvascular density near the skin and strong interference from stromal structures, such as tendons and bones. This scarcity accentuates optical instability and makes baseline stabilization difficult (Kiselev et al., 2024).
- **Peripheral vasomotor dynamics:** In locations distant from the hemodynamic center and under the effect of accentuated hydrostatic pressure, the optical signal begins to incorporate fluctuations in local vascular tone and venous return, blending central commands with a complex peripheral response (Kiselev et al., 2024; Charlton et al., 2022).

Therefore, it can be concluded that pulse and ankle readings are not interchangeable measures of the same physiological quantity. In scenarios where access to the upper limb is restricted, such as in patients with injuries or undergoing clinical interventions, ankle data should not be interpreted as direct estimates of central cardiac activity, but rather as reflections of localized peripheral hemodynamic dynamics.

4.3 The methodological scope of cubic interpolation: readability versus intrinsic validity

The comparative analysis between the raw and processed traces revealed a significant attenuation of acquisition noise, resulting in a visually homogeneous signal. However, from a methodological point of view, this smoothing serves an essentially geometric function. Cubic interpolation facilitates visual inspection and allows numerical convergence in statistical algorithms, but it does not, by itself, confer intrinsic validity to the measurements, the verification of which would require the establishment of an external reference standard.

This distinction is particularly relevant in the analysis of Heart Rate Variability (HRV). Although interpolation makes tracings numerically tractable and stable for subsequent calculations, excessive attenuation carries the risk of suppressing rapid and transient microvariations with real biological significance. Consequently, the procedure should be interpreted strictly as a tool for optimizing graphical readability, and not as a substitute for the original physiological dynamics a critical aspect in the evaluation of short-term indices, such as RMSSD and pNN50.

4.4 Considerations regarding the sample and the proportion of interpolated data

Finally, in accordance with the study's methodological criteria, it is noted that the entire sample of 30 participants was maintained in the final statistical analysis. The protocol adopted a strict cutoff threshold of 3 seconds for continuous failures and a 20% variation filter to isolate ectopic beats, ensuring that the proportion of data modified by cubic spline interpolation was minimal. This low incidence of gap filling ensures that the impact on short-term measurements was reduced, preserving the robustness of the conclusions without compromising the original dynamics of the RR interval time series.

4.5 The interface as an audit mechanism

In addition to smoothing, the interface functions as a quality control tool and reduces confounding factors in experimental protocols. This methodological value is demonstrated by the unequivocal detection of the mechanical artifact in the S2 sensor caused by the sphygmomanometer. Far from being a computational error, the interface's ability to discriminate and record this external instability demonstrates its usefulness as a real-time data auditing mechanism. This traceability allows the researcher to separate environmental or instrumental noise from genuine hemodynamic responses, ensuring the replicability and analytical rigor required in high-precision experimental work.

This is, in our opinion, the most transferable contribution of the study. The specific finding that ankle positioning degrades PPG quality is not physiologically surprising; what the platform adds is that the degradation was localized, recorded in terms of time, and attributed to its cause while the recording was still in progress, and that a second artifact of entirely different origin was distinguished from it. In a conventional post-hoc workflow, both would likely have been aggregated as unexplained missing data.

4.6 Limitations

Multichannel electrocardiography remains the clinical gold standard for recording cardiac activity and deriving HRV (heart rate variability). This study utilized the Samsung Galaxy Watch 4, a decision motivated by ecological validity and the objective of evaluating the technical feasibility of accessible mobile health tools. The following limitations apply.

- There is no concomitant reference standard. In the absence of simultaneous ECG, the analysis is limited to the consistency between the recordings from the wearable devices and comparison

with published validation literature; it is not possible to establish absolute clinical accuracy. Given the strong correlation reported between PPG sensors and conventional resting ECG, the results presented here should be interpreted in the context of continuous portable monitoring, and not as a definitive clinical diagnosis.

- Model and manufacturer of a single device. All three units were Samsung Galaxy Watch 4 devices; conclusions about placement may not apply to other sensor geometries or optical configurations.
- Only low-intensity activities. Walking at 1.5 km/h generates a narrow heart rate range; behavior at higher intensities, where the motion artifact is greater, was not examined.
- The location and identity of the device are not separate. Because each device occupied a fixed location, the specific hardware variation of the device cannot be formally distinguished from the effect of location.
- Healthy adult volunteers. It remains to be seen whether these results apply to elderly individuals or to patients with compromised peripheral perfusion, arrhythmia, or diabetes precisely the populations in which remote monitoring is most clinically valuable.

4.7 Future work

Three extensions follow directly from this. First, simultaneous ECG recording would convert the present consistency analysis into a validation study and allow for the quantification of absolute accuracy by positioning. Second, extending acquisition to devices from different manufacturers would test whether the interface integration layer generalizes beyond a single vendor ecosystem, which is the main claim of clinical relevance. Third, prospective implementation in a population

of patients in free-living conditions would establish whether the real-time audit mechanism retains its value outside of a supervised laboratory protocol.

5. Conclusion

This study developed a graphical interface that centralizes and processes physiological data from multiple smartwatches in real time. The results indicate that data fragmentation and sensor hardware limitations can be substantially mitigated by a robust software layer. Cubic interpolation made the noisy raw tracings readable and numerically tractable; as argued in Section 4.3, it improves the readability and stability of subsequent calculations, rather than the intrinsic validity of the measurements, which would require establishing a reference standard.

The comparison between acquisition sites revealed the study's main substantial finding: the fixation site is crucial for signal quality. Wrist recordings were more consistent, while ankle measurements showed marked unpredictability. The deviation from normality at S3 is not an instrumental error, but rather a consequence of this anatomical location: at the ankle, the PPG signal fails to faithfully track the central heart rhythm and instead captures a complex, localized, and unpredictable peripheral hemodynamic dynamic. The interface was able to identify anomalies and failures that would have gone unnoticed in a single acquisition, indicating that standardization of the usage protocol is as important as the accuracy of the algorithm.

The platform, therefore, does more than simplify simultaneous monitoring: it establishes a methodological basis upon which wearable devices can go beyond recreational use, becoming viable tools for scientific research and cardiovascular monitoring during activities of daily living. The contribution consists of an acquisition layer in which data from wearable devices in multiple locations are synchronized, inspectable, and traceable to the origin of each anomaly.

Statements

Ethical approval.

The study was conducted in accordance with the Declaration of Helsinki and approved by the Research Ethics Committee of the University of Mogi das Cruzes (CAAE: 82084924.9.0000.5497; opinion no. 7.117.006). Written informed consent (TCLE) was formally obtained from all participants prior to inclusion in the study.

Informed consent.

Free and informed written consent was obtained from all individual participants included in the study.

Conflicts of interest.

The authors declare that there are no financial or personal conflicts of interest that may have influenced the work reported in this article. No financial compensation or funding was received for the development of the graphical interface.

Financing.

This work was supported by the Coordination for the Improvement of Higher Education Personnel of Brazil (CAPES), Financial Code 001 (doctoral scholarship). Additional support was provided by the São Paulo Research Foundation (FAPESP), grant no. 21/14231-0.

Contributions from the authors.

Authors' contribution statement (CRediT)

- **Alexandre:** Conceptualization, Methodology, Software, Formal Analysis, Research, Writing, Original Draft, Writing, Revision and Editing.

- **Daniel:** Conceptualization, Methodology, Writing, Review and editing, Supervision, Obtaining funding.

Financing

This work was carried out with the support of a doctoral scholarship from the Coordination for the Improvement of Higher Education Personnel - Brazil (CAPES) - Funding Code 001. This work was also carried out with the support of process no. 21/14231-0, from the São Paulo Research Foundation (FAPESP).

Data Availability Statement

The datasets generated and analyzed in this study consist of anonymized human physiological data, used exclusively for statistical analyses and approved by the institutional Research Ethics Committee. Due to strict institutional privacy, ethics, and confidentiality policies regarding human data, the datasets are strictly unavailable for public release or external sharing and cannot be provided upon request.

Software Availability

The source code of the graphical interface developed in this study is legally protected under a patent held by the National Institute for Space Research (INPE, Brazil). Case No. BR512025003313-3In strict accordance with the institution's intellectual property regulations and patent protection policies, the source code cannot be deposited in publicly open access repositories or shared externally.

List of Figures and Tables

Figure 1 - Integrated architecture workflow: data acquisition via smartwatches (S1, S2, S3), Wi-Fi transmission, MySQL database storage, and analytical processing in Python via PyBios.

Source: Own elaboration (2024).

Figure 2A - Schematic representation of Stage I (seated rest, treadmill walking at 1.5 km/h, and seated recovery). Sensor S1 is placed on the right wrist and S3 on the left ankle; sensor S2 (left wrist) is located on the contralateral side.

Source: Own elaboration (2024).

Figure 2B - Schematic representation of Stage II (supine rest, treadmill walking at 1.5 km/h, and supine recovery). Sensor positioning follows the protocol shown in Figure 2A.

Source: Own elaboration (2024).

Figure 3 - Graphical user interface for real-time data collection. The top panel (blue) manages recording, buffer clearing, visualization, and custom file export; the status bar (green) shows operational state; the main table displays incoming multi-device streams including sensor/profile IDs, triaxial acceleration, rotation, gravity, heart rate metrics, and timestamps.

Source: Own elaboration (2024).

Figure 4 - Raw vs. cubic spline-smoothed heart rate signals. Raw photoplethysmography data (left) compared to the smoothed overlay (right). Cubic spline interpolation reduces high-frequency fluctuations to enhance visual inspection and numerical stability without altering the underlying physiological dynamics.

Source: Own elaboration (2024).

Figure 5 - Cubic spline interpolation applied to inter-beat RR intervals to reconstruct transient signal discontinuities and temporary data loss.

Source: Own elaboration (2024).

Table 1 - Descriptive statistics and Shapiro-Wilk normality test results for sensors S1, S2, and S3 during Stage I (seated rest, walking, and seated recovery).

Source: Own elaboration (2024).

Table 2 - Descriptive statistics and Shapiro-Wilk normality test results for sensors S1, S2, and S3 during Stage II (supine rest, walking, and supine recovery).

Source: Own elaboration (2024).

Table 3 - Sample of structured multi-device data ingested by the platform (idw4_sensores), including hardware/profile IDs, triaxial accelerometer, gyroscope, gravity vectors, heart rate status, BPM, and timestamps.

Source: Own elaboration (2024).

Declarations

- Clinical trial number: Not applicable.

References

[1] Hall JE, Guyton AC. Guyton and Hall Textbook of Medical Physiology. 13th ed. Philadelphia: Elsevier; 2017. (Cited in Section 1 - Introduction, when discussing the modulation of the autonomic nervous system on heart rate and HRV).

[2] Babu M, Lautman Z, Lin X, Sobota MHB, Snyder MP. Wearable devices: implications for precision medicine and the future of healthcare. Annu Rev Med. 2024;75:401–15.https://doi.org/10.1146/annurev-med-052422-020437(Cited in Section 1 - Introduction, regarding the proliferation of smartwatches outside the laboratory environment).

[3] Charlton PH, Allen J, Bailón R, Baker S, Behar JA, Chen F, et al. The 2023 wearable photoplethysmography roadmap. Physiol Meas. 2023;44(11):111001.https://doi.org/10.1088/1361-6579/acfc73(Cited in Section 4.2 - Discussion, when explaining the factors of pulse wave attenuation and viscoelastic damping in the lower limb).

[4] Muzny M, Henriksen A, Giordanengo A, et al. Wearable sensors with data exchange capabilities: analyzing the current state and needs of different actors in mobile health monitoring systems. Int J Med Inform. 2020;133:104017.https://doi.org/10.1016/j.ijmedinf.2019.104017(Cited in Section 1 - Introduction, addressing the data fragmentation inherent in wearable device ecosystems).

[5] Sarhaddi F, Kazemi K, Azimi I, et al. A comprehensive assessment of heart rate accuracy and heart rate variability in Samsung smartwatches. PLoS One. 2022;17(12):e0268361.https://doi.org/10.1371/journal.pone.0268361(Cited in Section 1.1 - Novelty and contribution of this work, regarding previous validation studies comparing wrist devices).

[6] Silva LEV, Fazan R, Marin-Neto JA. PyBioS: a free software for cardiovascular signal analysis. Comput Methods Programs Biomed. 2020;197:105718.https://doi.org/10.1016/j.cmpb.2020.105718(Cited in the Abstract and in Section 2.1 - Development of the graphical interface, regarding the processing and calculation of HRV indices).

[7] Kiselev AR, Posnenkova OM, Karavaev AS, et al. Frequency domain characteristics and low-frequency synchronization of photoplethysmographic waveform variability and heart rate variability with increasing cardiovascular disease severity. Biomedicines. 2024;12(9):2088.https://doi.org/10.3390/biomedicines12092088(Cited in Section 4.2 - Discussion, referencing capillary density, optical coupling, and peripheral vasomotor dynamics).

[8] The jamovi project. jamovi (Version 2.5) [Computer Software]. 2024. Available from:https://www.jamovi.org(Cited in Section 2.6 - Data processing and analysis, regarding the statistical support used in the study).